Diazoxide enhances excitotoxicity-induced neurogenesis and attenuates neurodegeneration in the rat non-neurogenic hippocampus.

Martínez-Moreno M[1], Batlle M[2], Ortega FJ[3], Gimeno-Bayón J, Andrade C, Mahy N, Rodríguez MJ

Departament de Biomedicina, Institut d'Investigacions Biomèdiques August Pi i Sunyer (IDIBAPS), Institut de Neurociències, Universitat de Barcelona and Centro de Investigación Biomédica en Red sobre Enfermedades Neurodegenerativas (CIBERNED), Barcelona, Spain

Author for correspondence: Dr. Manuel J. Rodríguez
Unitat de Bioquímica i Biologia Molecular
Dept. Biomedicina
Facultat de Medicina, UB
c/ Casanova 143
E-08036 Barcelona, SPAIN
Phone: +34 93 402 0586
FAX: +34 93 403 5882
E-mail: marodriguez@ub.edu

RUNING TITLE: Diazoxide enhances NMDA-induced neurogenesis

[1] Current Address: Molecular Neuroscience Laboratory, Weis Center for Research, Geisinger Clinic, 100 North Academy Avenue, Danville, Pennsylvania 17822, USA.

[2] Current address: Intensive Medicine Unit, Corporació Sanitària Universitària Parc Taulí, 08208 Sabadell, Spain.

[3] Current address: Vall d'Hebron Research Institute, Universitat Autònoma de Barcelona and Instituto de Salud Carlos III, Biomedical Network Research Centre on Rare Diseases (CIBERER), Pg Vall d'Hebron 119, 08035 Barcelona, Spain

ABSTRACT

Diazoxide, a well-known mitochondrial K_{ATP} channel opener with neuroprotective effects, has been proposed for the effective and safe treatment of neuroinflammation. To test whether diazoxide affects the neurogenesis associated with excitotoxicity in brain injury, we induced lesions by injecting excitotoxic N-Methyl-D-Aspartate (NMDA) into the rat hippocampus and analyzed the effects of a daily oral administration of diazoxide on the induced lesion. Specific glial and neuronal staining showed that NMDA elicited a strong glial reaction associated with progressive neuronal loss in the whole hippocampal formation. Doublecortin immunohistochemistry and bromo-deoxyuridine (BrdU)-NeuN double immunohistochemistry revealed that NMDA also induced cell proliferation and neurogenesis in the lesioned non-neurogenic hippocampus. Furthermore, glial fibrillary acidic protein (GFAP)-positive cells in the injured hippocampus expressed transcription factor Sp8 indicating that the excitotoxic lesion elicited the migration of progenitors from the subventricular zone and/or the reprograming of reactive astrocytes. Diazoxide treatment attenuated the NMDA-induced hippocampal injury in rats, as demonstrated by decreases in the size of the lesion, neuronal loss and microglial reaction. Diazoxide also increased the number of BrdU/NeuN double-stained cells and elevated the number of Sp8-positive cells in the lesioned hippocampus. These results indicate a role for K_{ATP} channel activation in regulating excitotoxicity-induced neurogenesis in brain injury.

KEYWORDS: Diazoxide; K_{ATP} channel; microglia; adult neurogenesis; neuroinflammation; tissue regeneration.

Adult neurogenesis occurs in delimited brain areas such as the subgranular zone (SGZ) of the dentate gyrus (DG) and the subventricular layer of the lateral ventricles (Lledo et al., 2006). This neurogenesis is associated with the presence of immature adult progenitor cells that have self-renewal capacity and can differentiate into one of the main neural cell types: neurons, astrocytes and oligodendrocytes (Lledo et al., 2006). Brain damage promotes neurogenesis in the SGZ of the DG and the subventricular zone (SVZ). Furthermore, injury or pathological stimuli are known to elicit the invasion and integration of newborn neurons into lesioned non-neurogenic regions. Following ischemia or brain trauma, proliferation increases in the SGZ of the DG (Kleindienst et al., 2005) and newborn neurons are also observed in the striatum and cortex (Bernier et al., 2002; Zhang et al., 2004; Ortega et al., 2013). The latter is attributed to the atypical migration of neuronal precursors from the SVZ towards the damaged areas and the activation of a latent neurogenic program in local astrocytes and parenchymal N2 glia (Péron and Berninger, 2015). The presence of newborn cell clusters in cortical areas close to blood vessels also suggests the recruitment of resident quiescent stem-like cells, or the infiltration of blood-borne cells (Zhang et al., 2004). Pathological conditions, therefore, trigger neurogenesis in central nervous system (CNS) regions where adult neurogenesis is usually non-existent.

Microglia are the primary immune effector cells in the brain that release factors promoting the proliferation, migration, and differentiation of precursor cells (Deierborg et al., 2010). When microglia become reactive in response to injury, they release pro-inflammatory cytokines that are generally anti-neurogenic. (Monje et al., 2003; Song and Wang, 2011; Ji et al., 2013; Mattei et al., 2014). However, microglia have been also reported to enhance neurogenesis under inflammatory conditions (Ekdahl et al., 2009; Sierra et al., 2014). Therefore, microglial activity depends on an equilibrium of the molecules secreted within the microenvironment (Salter and Beggs, 2014). Based on this theory, pharmacological control of microglial activation, which has been proposed to provide neuroprotection against neuroinflammation (Chen and Trapp, 2016), should also regulate the microglial influence on neurogenesic processes.

Ion channels expressed by microglia modulate cell functions and directly regulate of microglial activity during injury (Stebbing et al., 2015). ATP-sensitive potassium (K_{ATP}) channels are postulated to be one of these channels controlling microglial activity (Ortega et al., 2012; Rodríguez et al., 2013). K_{ATP} channels are hetero-octameric complexes composed of four regulatory sulfonylurea receptor (SURx)

subunits and four pore-forming inwardly-rectifying potassium (Kir6.x) subunits (Proks and Ashcroft, 2009). They act as metabolic sensors that regulate potassium flux and couple membrane excitability to cellular energy metabolism. K_{ATP} channels are also located on the mitochondrial inner membrane, where they participate in the control of mitochondrial volume and ATP synthesis (Cancherini et al., 2003). It is clear that K_{ATP} channel is a major component of the inflammatory response following brain injury. We and others have demonstrated that it regulates the reactive state of microglia, controls the release of inflammatory mediators, such as nitric oxide (NO) and tumor necrosis factor-alpha (TNFα), and modifies phagocytic activity (Zhou et al., 2008; Virgili et al., 2011; Ortega et al., 2012). Despite these findings, the role of K_{ATP} channel in the neurogenesis associated with inflammatory conditions is still largely unknown. Diazoxide (7-chloro-3-methyl-4H-1,2,4-benzothiadiazine 1,1-dioxide; Dzx) is a well-known drug that opens K_{ATP} channels showing high affinity for mitochondrial K_{ATP} (mito K_{ATP}) channels (Ashcroft and Gribble, 2000; Rodríguez et al., 2013). Dzx activates K_{ATP} channels in pancreatic β cells and the smooth muscle of blood vessels, which results in the inhibition of insulin secretion and vasorelaxation (Richer et al., 1990; Petit and Loubatières-Mariani, 1992) and a subsequent increase in the plasma glucose concentration. Because of that, Dzx has been approved and used since the 1970s for treating malignant hypertension and hypoglycemia (Koch-Weser, 1976). Oral Dzx crosses the blood brain barrier (Kishore et al., 2011) and exerts neuroprotective effects in the CNS. Previous studies have demonstrated that oral administration of Dzx ameliorates disease progression and causes neuroprotection in animal models of Alzheimer's disease and multiple sclerosis (Liu et al., 2010; Virgili et al., 2011). Furthermore, Dzx can exert neuroprotective effects on the brain against ischemia, trauma, and neurotoxicants (Roseborough et al., 2006; Robin et al., 2011; Shukry et al., 2015). These results indicate novel roles for Dzx as a glia-mediated anti-inflammatory and neuroprotective agent. Here, we tested our hypothesis that Dzx modifies the microglial influence on the neurogenesis induced by brain damage using an *in vivo* experimental model of neurodegeneration that impairs performance in learning-memory tasks (Bardgett et al., 2003). We stereotaxically microinjected N-methyl-D-aspartate (NMDA) into the rat hippocampal formation (HF) to induce a neurodegenerative process triggering a potent microglia-mediated inflammatory reaction (Rodríguez et al., 2013; Batlle et al., 2015; Espinosa-Parrilla et al., 2015). We then orally administered Dzx and analyzed any changes in lesion-induced neuroinflammation and neurogenesis.

Our results indicated that Dzx reduced NMDA-induced neuroinflammation and enhanced neurogenesis in the HF.

EXPERIMENTAL PROCEDURES

Animals and materials

Adult male Wistar rats were obtained from the animal housing facilities of the School of Medicine (Universitat de Barcelona). Rats weighed 200-225 g at the beginning of the study and were housed with free access to food and water on a 12/12 hour light/dark cycle. Animals were manipulated according to the European Communities Council Directive of 24 November 1986 (86/609/EEC). For sufficient statistical power, we estimated that 6 rats should be included in each group (tolerance interval ± 0.9, confidence level 95%). Great efforts were made to minimize the number of animals used and their suffering. Procedures were approved by the Ethics Committee of the Universitat de Barcelona, under supervision of the local authorities.

NMDA, Dzx, dimethyl sulfoxide (DMSO), diaminobenzidine (DAB), bromo-deoxyuridine (BrdU), mouse monoclonal anti-glial fibrillary acidic protein (anti-GFAP) antibody, biotin-conjugated isolectin B4 (IB4) from *Bandeiraea simplicifolia*, and TRI Reagent® RNA isolation reagent were purchased from Sigma (St. Louis, MO, USA). Rat monoclonal anti-BrdU antibody was purchased from Immunologicals Direct (Oxford, UK); mouse monoclonal anti-NeuN antibody from Millipore (Boston, USA), and goat monoclonal anti-doublecortin (DCX) antibody was obtained from Santa Cruz Biotechnology (Santa Cruz, CA). Rabbit polyclonal anti-Sp8 antibody was purchased from Millipore (Boston, USA). Immunohistochemical reagents and secondary peroxidase-conjugated antibodies were purchased from Sigma, and the different fluorophorus-conjugated antibodies were purchased from Invitrogen (Carlsbad, CA, USA). The First Strand cDNA Synthesis kit was from Fermentas (St. Leon-Rot, Germany), whilst the SensiFAST™ SYBR No-ROX One-Step mix was purchased from Applied Biosystems (Foster, CA). PCR primers for the target genes were obtained from RealTimePrimers (Elkins Park PA, USA).

Stereotaxic procedure and treatment of rats

The stereotaxic procedure was performed as previously described (Batlle et al., 2015; Espinosa Parrilla et al., 2015). Briefly, rats were anesthetized with equithesin and

placed in a stereotaxic instrument (David Kopf, Carnegie Medicin, Sweden) with the incisor bar set at -3.3 mm. The stereotaxic coordinates were 3.3 mm caudal to bregma, 2.2 mm lateral to bregma, and 2.9 mm ventral from dura, according to the Atlas of Paxinos and Watson (1986). For the unilateral intracerebral injection into the hippocampal parenchyma, we used a 5.0-µl Hamilton syringe and an infusion pump (CMA/100; Carnegie Medicin, Sweden). A volume of 0.5 µl was injected over 5 minutes. Rats received either a single microinjection of 20 nmol NMDA diluted in 50 mM phosphate buffered saline (PBS; pH 7.4) (NMDA group) or a microinjection of 50 mM PBS (pH 7.4) (sham group).

To study the effects of Dzx, this drug was administered daily *per os* from the 8th day until the day of sacrifice using an animal-feeding needle of size 76.2 mm from Harvard Apparatus (Holliston, MA, USA). Some rats were administered either 1 mg/kg Dzx (treated group) or diluent (0.3% DMSO in water, vehicle group). A total of 120 rats were distributed into the following groups (12 rats per group): Sham rats (sacrificed on days 5, 15 or 38 post-injection); Sham + Dzx rats (sacrificed on day 15 post-injection, treated with Dzx for 7 days, or sacrificed on day 38 post-injection, treated with Dzx for 30 days); NMDA 5 days (sacrificed on day 5 post-lesion); NMDA 15 days (sacrificed on day 15 post-lesion); NMDA 38 days (sacrificed on day 38 post-lesion) NMDA 15 days + Dzx (sacrificed at post-lesion day 15, treated with Dzx for 7 days) NMDA 38 days + Dzx (sacrificed on day 38 post-lesion, treated with Dzx for 30 days). Half of the animals (6 rats in each group) were used for biochemical studies and the other half were used for histological investigations (Figure 1). The Dzx and NMDA doses were chosen according to previous studies (Virgili et al., 2011; Rodríguez et al., 2013; Batlle et al., 2015).

To determine the effects of Dzx treatment on glycaemia, we monitored blood glucose levels in NMDA+Dzx rats before and 2 hours after Dzx treatment, every two days. Glucose measurements were performed using an Accu-ChekTM Aviva glucometer (Roche Diagnostics, Basel, Switzerland). Blood samples were obtained from the distal part of the tail. According to the animal welfare guidelines, glucose concentrations higher than 176 mg/dL were considered hyperglycemic. The selected Dzx dose did not affect glycemia in rats (Figure 2A). As they were used at low concentrations, the anesthetics did not interfere with the function of the NMDA receptors (Batlle et al., 2015).

To determine the proliferation peak induced by the NMDA injection into the rat hippocampus, 6 sham and 6 NMDA rats received an intraperitoneal injection of BrdU (50 mg/Kg in 50 mM PBS) on different starting days after toxin injection (from day 1 to day 4, day 4 to 8, 8 to 12, and 12 to 15) (Figure 1A). All rats were sacrificed 15 days post-lesion by transcardial perfusion of 4% paraformaldehyde. Cell proliferation was assessed by BrdU immunohistochemistry and cells were stereologically counted using the optical fractionator method (see bellow). Once the time of the proliferation peak was determined (Figure 2B), all rats sacrificed on day 15 or 38 post-lesion received an intraperitoneal injection of BrdU (50 mg/Kg in 50 mM PBS) from day 4 to day 8 post-lesion. The fate of the newly generated cells at the proliferation peak was examined in the group of animals sacrificed 30 days after the last BrdU injection (day 38 post-lesion).

Real-time RT-PCR

At the indicated post-lesion time (Figure 1B), 6 rats from each group were anaesthetized and decapitated. The brain was then removed and the HF dissected, before being quickly frozen in liquid N_2 and stored at -80°C prior to use. Total RNA was isolated using the TRIzol reagent (Invitrogen, Paisley, UK), following manufacturer's instructions. We synthesized 2 µg of first-strand cDNA with random primers using the First Strand cDNA Synthesis kit. The RT reaction was performed at 42°C for 60 minutes followed by 5 minutes at 70°C. Real-time PCR was conducted using the SensiFAST^{TM} SYBR No-ROX One-Step mix according to manufacturer's instructions. The PCR program was: 2 minutes at 95°C for denaturation; 45 cycles of 15 seconds at 95°C for amplification and 1 minute at 60°C for final extension. For each target gene, the expression level was normalized to the mRNA level of GAPD. Primer sequences for target gene and endogenous controls are presented in Table 1. The ΔΔCT method was used to analyze the data as described by Bookout et al. (2006).

Histology, immunohistochemistry, and image analysis

After anesthesia, rats were transcardially perfused with 300 ml of 0.01 M PBS followed by 300 ml of 4% (w/v) paraformaldehyde in 0.01 M phosphate buffer (PB). The brains were removed, post-fixed, and transferred to 15% (w/v) sucrose in PB at 4ºC. The brains were then frozen with powdered dry ice and stored at -80ºC until use. Eight series of 25 adjacent 14-µm coronal sections from the whole hippocampus were obtained from the brains and mounted on poly-L-lysine-pretreated slides (10% w/v in distilled water).

Standard Nissl staining was performed to evaluate the areas of neuronal loss and the morphometry of the HF. Microglial cells were labeled for isolectin B4 (Rodríguez et al., 2009). Briefly, sections were incubated overnight at 4ºC with IB4 diluted at 1:25 in normal goat serum (NGS, 1:100 v/v in 0.01 M PBS; pH 7.4). Then, they were incubated with ExtrAvidin (1:250) and developed in a 0.05-M Tris solution containing 0.03% (w/v) DAB and 0.006% (v/v) H_2O_2.

Immunohistochemistry was carried out as previously described (Rodríguez et al., 2004) using the biotin-avidin-peroxidase method. Anti-GFAP antibodies were used to assess astroglial reactivity. Neuronal staining was undertaken with the anti-NeuN antibody, and the study of immature neurons performed with the anti-DCX and anti-Sp8 antibodies. Briefly, sections were incubated overnight at 4ºC with the primary antibody diluted in NGS at the appropriate concentration. After incubation with the appropriate biotinylated secondary antibody, sections were incubated with ExtrAvidin and developed in DAB and H_2O_2. Proliferating cells and their progeny were detected by BrdU incorporation into the DNA of cells in the S-phase of the cell cycle (Nowakowski et al., 1989). BrdU was detected using mouse monoclonal anti-BrdU antibody. After DNA denaturation with 2M HCl at 37 ºC and incubation with 0.1M boric acid in 0.01M PBS, pH 8.5, sections were incubated overnight at 4ºC with the rat monoclonal anti-BrdU antibody diluted at 1:100 (v/v) in NGS. After incubation with biotinylated mouse anti-rat antibody (1:100), sections were incubated with ExtrAvidin (1:250), and developed in DAB and H_2O_2.

The fate of the new proliferating cells was determined by double immunohistochemical staining with BrdU and specific cellular markers (Figure 1C). After DNA denaturation with 2M HCl at 37ºC and incubation with 0.1M boric acid in 0.01M PBS, pH 8.5, sections were co-incubated overnight at 4ºC with the rat monoclonal anti-BrdU antibody and one of the following antibodies: mouse monoclonal anti-GFAP antibody for astroglial cells; mouse monoclonal anti-NeuN antibody for neurons; or goat monoclonal anti-DCX for immature neurons. For GFAP and NeuN, sections were then sequentially incubated in the dark with biotinylated mouse anti-rat IgG (1:100), FITC-conjugated), ExtrAvidin (1:250), and finally goat anti-mouse antibody conjugated with Alexa Fluor-555 (1:100). For DCX, sections were sequentially incubated with biotinylated mouse anti-rat IgG (1:100) and then with donkey anti-goat-IgG conjugated with Alexa Fluor-488 (1:100) and Cy3-conjugated ExtrAvidin (1:100). To determine the microglial phenotype of the newly generated cells sections were co-incubated

overnight at 4ºC with the rat monoclonal anti-BrdU antibody and the biotinylated IB4. Sections were then sequentially incubated in the dark with Cy3-conjugated ExtrAvidin (1:250) to label biotinylated IB4, and with biotinylated mouse anti-rat antibody (1:100) followed by FITC-conjugated ExtrAvidin (1:250) to detect BrdU. All sections were mounted in ProLong antifade mountant and kept in the dark. Incubations with either goat or mouse IgG as primary antibodies were used for negative controls. A Leica TCS SL laser scanning confocal microscope (Leica Microsystems Heidelberg GmbH, Manheim, Germany) was used to acquire confocal images.

The hippocampal size, different hippocampal subfield areas, and areas showing neuronal loss were measured on Nissl-stained sections using the Image-Pro Plus image analysis software (Media Cybernetics Inc., MD, USA). Microglial and astroglial reaction areas were measured in IB4-stained and GFAP-immunostained sections, respectively, using the same software. In all cases, the area of contralateral hippocampus was measured to estimate the effects of histological procedures on tissue size and, thus, to correct for individual variability in brain size and tissue shrinkage.

Stereological counting of proliferating cells was performed on sections stained for BrdU and on sections double-stained for BrdU and either GFAP, IB4, NeuN, or DCX. We applied the optical fractionator method to count labeled cells, as previously described (Ortega et al., 2013). Lesioned regions of the HF were identified under 2.5x magnification on arbitrary uniform random (AUR) coronal sections. For cell counting, we used the Mercator Pro 7.0 software (ExploraNova, france) to select AUR-sampled sites, and individual cells were viewed and counted under 40x magnification.

Confocal images were acquired using a Leica TCS SL laser scanning spectral confocal microscope. Co-localization of fluorescent labeling in the hippocampus was analyzed in single confocal images, as published elsewhere (Espinosa-Parrilla et al., 2015). Briefly, for each image, the map showing the spatial distribution of normalized mean deviation product (MDP) values (Jaskolski et al., 2005) and the scatter plot of pixel distribution were obtained and analyzed. The co-localization study also included the determination of Pearson's "r" coefficient, the overlap coefficient R, and the overlap coefficients for the green (k1) and red (k2) channels. All image analyses were performed with FluoColoc (ExploraNova, France) and ImageJ software.

Statistical analysis

For each parameter, the normal distribution of data was tested analyzing Kurtosis and Skewness moments. Statistical analysis was performed using a one-way analysis of variance (ANOVA), followed by Bonferroni's *post hoc* test for pairwise group comparisons. Values are presented as mean ± standard error of the mean (SEM), with significance determined at $P<0.05$. Neuronal loss is expressed as values relative to those of the sham group. All analyses were performed with the statistic package STATGRAPHICS (STSC Inc., Rockville, MD, USA).

RESULTS

Diazoxide attenuates the NMDA-induced neurodegenerative process in the rat hippocampus

In our previous study (Rodríguez et al., 2013) we showed that activated microglia expressed K_{ATP} channels in the rat NMDA-lesioned hippocampus. To monitor this microglial expression, here, we quantified by RT-qPCR the mRNA levels of Kir6.1, Kir6.2, SUR1 and SUR2 in the hippocampus of sham and NMDA-lesioned rats at different post-lesion times. We also analyzed the effects of Dzx on these expression levels (Table 2). Compared to sham rats, we found significant increases in Kir6.1 (2.59-fold; $p = 0.009$) and SUR2 (2.21-fold; $p = 0.007$) expression 5 days after the NMDA injection. This increase in expression was not significant at longer times after lesion induction. Dzx significantly increased SUR2 expression only on day 38 post-lesion (2.47-fold; $p = 0.046$; Table 2).

We then studied the long-term effects of chronic Dzx oral administration on excitotoxicity-induced neurodegeneration. Inspections of Nissl-stained sections revealed that 20 nmol NMDA produced major disorganization, neuronal loss and gliosis in all the layers of the HF. A daily dose of 1 mg/kg/day Dxz attenuated these NMDA-induced effects on days 15 and 38 post-lesion (Figure 3A-C). We measured morphological changes in the lesioned hippocampal area using Nissl-stained sections. We noted that 50 mM PBS microinjection caused no significant lesion in the hippocampus except for the needle puncture wound, at any of the four studied time points (Figure 3G). By contrast, 20 nmol NMDA induced a progressive increase in the lesioned area that reached a maximal size covering 41 ± 5% of the whole hippocampus 38 days after lesion induction ($p = 0.0004$). This area of the lesion was 24 ± 3% smaller ($p = 0.015$) in the hippocampus of NMDA-lesioned rats receiving a daily dose of Dzx (Figure 3G).

We then assessed the area of NMDA-induced neuronal loss in the pyramidal CA and granular DG layers of NeuN-immunostained HF (Figure 3D-F). In NMDA rats, the area of neuronal loss covered 28 ± 7% of the pyramidal CA1 and CA2 layers 5 days post-lesion, progressively reaching a maximal value of 71 ± 9% on day 38 post-lesion ($p = 0.0099$). Dzx treatment decreased this area of neuronal loss by 31 ± 4% on day15 post-lesion; however there was no significant effect on day 38 post-lesion (figure 3H). In the granular layer of the DG, Dzx reduced the area of NMDA-induced neuronal loss by 42 ± 8% on day 15 post-lesion ($p = 0.0450$), this decrease remaining significant on day 38 post-lesion (Figure 3I).

We studied microglial reaction by IB4 histochemistry (Figure 4A-C). Whilst there was no significant microglial reaction in sham rats, except that associated with the needle puncture wound, NMDA induced microglial reactivity covering 36.50 ± 4.33% of the total hippocampal area on day 5 post-lesion ($p = 0.0005$). This area increased with time to reach a maximal value of 61 ± 7% of the whole HF on day 15 post-lesion (Figure 4G), slightly decreasing on day 38 post-lesion. Dzx treatment significantly reduced this microglial reaction area to the 33 ± 5% of the whole hippocampus on day 15 (reduction of 47 ± 6%; $p = 0.0032$), which remained decreased on day 38 post-lesion (Figure 4G).

The area of NMDA-induced astrogliosis was assessed by GFAP-immunohistochemistry (Figure 4D-F). In sham animals, this area was restricted to the needle puncture wound, reaching a maximal value of 6.5 ± 4% of the whole hippocampal area 5 days post-lesion (Figure 4H). We detected reactive astrocytes in 24.36 ± 5.69% of the hippocampal area 5 days after NMDA microinjection. This area of astrogliosis reached a maximal size of 49 ± 4% on day 15 post-lesion ($p = 0.0005$), slightly decreasing on day 38 post-lesion. Dzx decreased the area of NMDA-induced astrogliosis by 26 ± 6% on day 15 post-lesion ($p = 0.0456$), this decrease remaining significant 38 days after lesion induction (Figure 4H).

Diazoxide enhances NMDA-induced neurogenesis in the rat hippocampus

NMDA induced cell proliferation in the hippocampus that reached a maximal value 4 to 8 days after lesion induction, as detected by BrdU immunohistochemistry (Figure 2B). To determine the cell type of the newly generated cells, we performed double immunohistochemical staining and confocal microscopy to identify cells stained with BrdU and a cell-specific marker 38 days post-lesion. BrdU-NeuN double-immunostained cells in the lesioned area accounted for 40 ± 3% of all the mitogenic

cells (Figure 5A). Of the cells co-expressiong BrdU and NeuN, 78 ± 5% were in the lesioned hippocampal parenchyma and CA layers, while only 22 ± 1% where in the DG (Figure 5B). Only 5.8 ± 0.7% of BrdU-positive cells displayed IB4 staining and were homogeneously distributed throughout the hippocampal lesioned area (Figure 5C-D). Meanwhile, 51 ± 4% of BrdU-positive cells were immunoreactive for GFAP. These cells were widely distributed throughout the entire hippocampal lesioned area, with only 3.7 ± 0.2% located in the DG (Figure 5E-F). Dzx treatment did not modify the number and distribution of BrdU-positive cells but did significantly affect cell fate (Figure 5G) since only 8.5 ± 1% of BrdU-positive cells were also immunoreactive for GFAP whereas the 32 ± 3% were positive for IB4 and the remaining 59.5 ± 7% immunopositive for NeuN (Figure 5B, D, F, G).

We monitored the location of DCX-immunostained cells to study the neurogenic time course in the lesioned area (Figure 6A-F). Sham animals displayed the same number of DCX-stained immature neurons within the SGZ during the course of the study. In NMDA-lesioned rats, DCX-positive cells were mainly scattered throughout the entire lesioned hippocampus (Figure 6G). When quantifying cells co-expressing BrdU and DCX, 75 ± 5% of DCX-positive cells were immunonegative for BrdU (Figure 6H). BrdU-DCX-positive cells were less abundant in the lesioned DG than in the SGZ and the lesioned hippocampus. Comparison of BrdU-DCX-positive cells 15 days post-lesion with BrdU-NeuN double-stained neurons 38 days post-lesion demostrated a 43% decrease in the area of the lesioned hippocampus (Figures 5B, 6H).

Diazoxide enhances the NMDA-induced presence of SP8-GFAP-positive cells in the hippocampus

As most neuroblasts and newly generated neurons were not mainly located in the DG, we evaluated their putative SVZ origin by immunohistochemically analyzing the transcription factor Sp8. Cells immunopositive for Sp8 were detected in the SVZ along the entire lateral wall of the ventricles, but there was no specific staining in the intact SGZ of the DG (Figure 7A, B) On day 15 post-lesion, Sp8 immunopositive cells were present in all the lesioned hippocampal subfields, mainly in the oriens and radiatum strata of CA1, the lacunosum moleculare, and the ventral part of the hippocampus near the thalamus (Figure 7C). These cells presented Sp8 staining in the nucleus and cytoplasm, some showing intense immunostaining in the cellular processes (Figure 7D). The numbers of Sp8-positive cells were similar in all the lesioned layers 38 days post-

lesion (Figure 7F). Dzx treatment showed no clear effect on hippocampal Sp8-immunolabeling 15 days post-lesion, but did increase the number of Sp8-positive cells by 103 ± 21% on day 38 post-lesion ($p = 0.0341$) (Figure 7G-I).
To determine whether these Sp8-positive cells were of neuronal or glial nature, we performed both Sp8-NeuN and Sp8-GFAP double immunostaining of hippocampal slices obtained from day 38 post-lesion. Confocal mmicroscopic analysis of cells stained with anti-Sp8 and anti-NeuN antibodies reveales that Sp8-positive cells were not neuronal. (Figure 8A - F), producing a mean Pearson's r value of 0.095 for the MDP images analyzed. Almost all the Sp8-positive cells were GFAP-immunopositive (Figure 8G - L), with a mean Pearson's r value of 0.34 for the red channel and 0.19 for the green channel.

DISCUSSION

K_{ATP} channel activators such as Dzx are well-known compounds approved for treating hypoglycemia and hypertension, with additional neuroprotective properties against ischemia, trauma, and neurotoxicants (Robin et al., 2011; Shukry et al., 2015). Recently, we and others have reported novel roles for Dzx as an anti-inflammatory agent, which could contribute to the neuroprotective effects. Dzx has been shown to prevent microglial TNFα, NO and interleukin-6 production after activation with different stimuli *in vitro* (Zhou et al., 2008; Virgili et al., 2011). Here, our in vivo results demonstrated that Dzx preserves neurons and decreases microglial reaction against an excitotoxic neurodegenerative insult, possibly through its anti-inflammatory action.
Different CNS cell types, including neurons (Humphries and Dart, 2015), oligodendrocytes (Fogal et al., 2010) and microglia (Virgili et al., 2011; Ortega et al., 2012), express K_{ATP} channels as a combination of Kir6.2 and SUR1 subunits. K_{ATP} channels are also expressed by endothelial cells, where they could be involved on the vascular response to physiological events (Rosenblum, 2003). Thus, Dzx not only acts on microglial cells, but also on other cell types in a dose-dependent manner. At the dose used in the present study (1 mg/kg/day) we found no effects of Dzx on peripheral glucose concentration, confirming the specificity of Dzx activity on CNS cells.
In our model, oral administration of Dzx at a low concentration (1mg/kg/day) preserved NMDA-induced cell death. Other studies in different animal models have shown that Dzx protects against cell death from excitotoxicity or inflammation, generating beneficial outcomes (Zhou et al., 2008; Liu et al., 2010; Virgili et al., 2011) and

modulating the innate immune response (Virgili et al., 2014).

The mechanisms underlying such actions of Dzx are not yet completely understood. Dzx-mediated neuroprotection is thought to be linked to the mitochondria, which are the main ATP-generating sites in the cell. Microglial activation involves a metabolic reprograming that leads to potentiation of anaerobic glycolysis (Gimeno-Bayón et al., 2014), higher numbers of mitochondria labeled with [^{3}H]PK11195 (Bernal et al., 2009) and increased mitoK_{ATP} channel expression (Rodríguez et al., 2013). Activation of mitoK_{ATP} channels increases potassium flux into the mitochondrial matrix and avoids excessive mitochondrial contraction that is deleterious for electron transport (Cancherini et al., 2003). Indeed, cells treated with Dzx demonstrate favorable energy profiles with limited damage following stress challenges (Iwai et al., 2000). Furthermore, Dzx has been reported to provide cardioprotection through mitoK_{ATP} activation (Henn et al., 2015). Thus, Dzx could exert its neuroprotective effects through increasing the ATP/ADP ratio in the mitochondria and cytoplasm of reactive microglia. If we consider the specific action of Dzx on plasmalemma K_{ATP} channels, K_{ATP} channel activity at the cell membrane would therefore be regulated by ATP-mediated inhibition and Dzx-induced activation (Rodríguez et al., 2013).

Our *in vivo* results revealed that NMDA-induced excitotoxicity increased the proliferation and maturation of newborn neurons in the lesioned HF. Many studies have described enhanced adult SGZ neurogenesis after acute injury such as ischemia, traumatic brain injury, experimentally induced epilepsy and trimethyltin intoxication (Corvino et al., 2005; Kleindienst et al., 2005; Hattiangady and Shetty, 2008). However, the induction of proliferation in those studies is not sustained long term and the number of newly generated neurons is limited. The reasons for this limited neurogenesis could be asymmetric or symmetric division of newborn cells leading to mature glial cells and the formation of the glial scar (Sofroniew, 2009; Sierra et al., 2015) or newly generated neurons hardly integrating into the hippocampal circuits and thus, degenerating (Sun et al., 2005). In any case, this neurogenesis eventually accelerates the depletion of the neural stem cell pool (Sierra et al., 2015; Zhang et al., 2015). However, here, we report a new finding of neuroblasts and newly generated neurons being detected in the lesioned HF by both DCX-immunohistochemistry and BrdU-NeuN double staining. Moreover, the expression of the transcription factor Sp8 by GFAP-positive cells in the injured hippocampus indicates that an excitotoxic lesion induces neurogenesis by eliciting the migration of progenitors from the SVZ and/or reprograming reactive

astrocytes in the lesioned HF.

Sp8-positive cells are the major population of olfactory bulb GABAergic interneurons constantly produced in the SVZ (Waclaw et al., 2006; Liu et al., 2009) and are not present in the SGZ of the DG. The presence of several Sp8-positive cells in the lesioned HF may reflect infiltration of blood-borne cells (Zhang et al., 2004). However, the Sp8-GFAP positive cells we found indicate either a robust recruitment of neuroblasts from the SVZ into the damaged hippocampus or reactive astrocytes acquiring progenitor cell properties after injury, as previously described for ischemic brain injury (Sirko et al., 2013). In either case the appearance of Sp8-positive neuroblasts in the lesioned hippocampus would compensate for the reduced neuroblast pool in the SGZ. It is important to point out that most DCX-positive cells were not immunopositive for BrdU, suggesting that migration or the appearance of these new neuroblasts in the damaged hippocampus is not preceded by the induction of cell proliferation. The constitutive expression of Sp8 by neuroblasts during the course of the study, which has been also observed in the striatum after stroke (Liu et al., 2009), indicates that the intrinsic differentiation program of adult neuroblasts is not altered by brain area-specific external factors or cerebral injury.

Our data indicate that neurogenesis is a microglial-dependent process, with microglia being required for controlling of progenitor cell migration and differentiation (Sato, 2015) and exacerbated microgliosis being detrimental for neurogenesis (Solano Fonseca et al., 2016). In the pathogenic brain, together with reactive astrocytes, microglia produce trophic factors that promote neurogenesis (Ribeiro Xavier et al., 2015) and inflammatory compounds that inhibit neurogenesis (Monje et al., 2003; Song and Wang, 2011; Ji et al., 2013; Mattei et al., 2014). Given that Dzx decreased chronic microglial reaction and the extent of the lesion in our model, and that *in vitro* Dzx attenuates the pro-inflammatory activity of reactive microglia (Zhou et al., 2008; Virgili et al., 2011), Dzx may promote neurogenesis by reducing the synthesis of inflammatory compounds. As there is no evidence of K_{ATP} channel expression in neuroblasts (Ortega et al., 2014), the effect of Dzx on neurogenesis could be through controlling microglial reactivity. Thus, by regulating the reactive phenotype of microglia through K_{ATP} channel activation, we Dzx increased the number of newly generated NeuN-positive cells and the occurrence of Sp8-GFAP-positive cells in the lesioned HF in the present study. The latter cells could have migrated from the pool located in the SVZ or from layers I and II of the cerebral cortex (Zhang et al., 2015). Whatever the case, the

mechanisms underlying microglial recruitment of these cells remain to be elucidated. Not all anti-inflammatory therapies may be beneficial for restoring neurogenesis. In a previous study, we demonstrated that blocking of microglial K_{ATP}-channels enhanced microglial release of MCP-1 and neurosphere proliferation, while partly affecting cell fate determination (Ortega et al., 2014). These results were consistent with those of other showing that neuroinflammation promotes neurogenesis. For example, anti-inflammatory treatment with minocycline does not affect neurogenesis (Ng et al., 2012), nor reduce proliferation of SVZ progenitors after inflammation (Deierborg et al., 2010). Furthermore, some inhibitors of cyclooxigenase-2, which is highly expressed by reactive microglia, are potent suppressors of neurogenesis (Goncalves et al., 2010). These findings reinforce the idea that some pro-inflammatory modulators do not inhibit adult neurogenesis. Thus, as microglial activation mediates inflammation at the site of injury (Domercq et al., 2013) and neuroblasts from the SVZ respond positively to inflammatory mediators (Ekdahl et al., 2009), therapies completely abrogating inflammation could be detrimental under certain conditions in regulating neurogenesis after injury. Thus, compounds like Dzx that modulate, but do not abolish, microglial inflammatory activity could be used to promote neurogenesis in cerebral damage. Newborn hippocampal neurons after ischemia have been reported to be partially functional three months after the injury and to ameliorate the induced neurological deficits in rats (Nakatomi et al., 2002). However, the fact that neuroblasts retain their SVZ phenotype during the course of the study may indicate an aberrant neurogenesis and impairment of hippocampal functioning, as described in pathological situations such as stress, depression and epilepsy (Ming and Song, 2011). It would be interesting to ascertain the role of the newly generated Sp8-positive cells in the injured HF, as they may act as newborn type II astrocytes or differentiate into neurons with the same function as those of hippocampal GABAergic interneurons (Zhang et al., 2015). If the latter is correct, this would reinforce the use of therapeutic approaches promoting the long-term capacity of the brain to regenerate hippocampal function in neurological disorders (Picard-Riera et al., 2004). However, the main degenerating cells in the injured hippocampus are glutamatergic pyramidal neurons, whose regeneration should be considered when developing therapies.

CONCLUSION

Our results provide clear evidence of the neuroprotective and anti-inflammatory effects of activating K_{ATP} channels during excitotoxicity in the rat hippocampus. We also demonstrate the role of K_{ATP} channel opening in controlling of excitotoxicity-induced neurogenesis. Whether the increased neurogenic response to Dzx is beneficial remains uncertain and further experiments are needed to solve this issue. If it were confirmed, regulating reactive microglial activity through pharmacologically manipulating of the K_{ATP}-channels could be used to curtail neuroinflammation and promote regeneration in the treatment of neurodegenerative diseases.

COMPETING INTERESTS

NM and MJR have applied for a PCT application "Diazoxide for use in the treatment of a central nervous system (CNS) autoimmune demyelinating disease" (application no. PCT/EP2011/050049). The other authors declare that they have no conflicts of interest.

7. AUTHORS CONTRIBUTIONS

MJR designed the study. NM & MJR obtained financial support for the study. MM-M, MB, FJO, JG-B & CA performed the experiments. MM-M, MB, NM & MJR analyzed and discussed the results. MM-M, NM & MJR wrote the manuscript. All authors have approved the final article.

8. ACKNOWLEDGMENTS

This research was supported by grant 2014SGR1115 from the Generalitat de Catalunya, Spain. The funder had no involvement in the study design, the collection, analysis and interpretation of data, the writing of the report, and in the decision to submit the article for publication.

BIBLIOGRAPHY

Ashcroft FM, Gribble FM (2000) New windows on the mechanism of action of K(ATP) channel openers. Trends Pharmacol Sci 21:439–445.

Bardgett M, Boeckman R, Krochmal D, Fernando H, Ahrens R, Csernansky J (2003) NMDA receptor blockade and hippocampal neuronal loss impair fear conditioning and position habit reversal in C57Bl/6 mice. Brain Res Bull 60:131–142.

Batlle M, Ferri L, Andrade C, Ortega F-J, Vidal-Taboada JM, Pugliese M, Mahy N, Rodríguez MJ (2015) Astroglia-Microglia Cross Talk during Neurodegeneration in the Rat Hippocampus. Biomed Res Int 2015:102419.

Bernal F, Petegnief V, Rodríguez MJ, Ursu G, Pugliese M, Mahy N (2009) Nimodipine inhibits TMB-8 potentiation of AMPA-induced hippocampal neurodegeneration. J Neurosci Res 87:1240–1249.

Bernier PJ, Bedard A, Vinet J, Levesque M, Parent A (2002) Newly generated neurons in the amygdala and adjoining cortex of adult primates. Proc Natl Acad Sci U S A 99:11464–11469.

Bookout AL, Cummins CL, Mangelsdorf DJ, Pesola JM, Kramer MF (2006) High-throughput real-time quantitative reverse transcription PCR. Curr Protoc Mol Biol Chapter 15:Unit 15.8.

Cancherini D V, Trabuco LG, Rebouças NA, Kowaltowski AJ (2003) ATP-sensitive K+ channels in renal mitochondria. Am J Physiol Renal Physiol 285:F1291–F1296.

Chen Z, Trapp BD (2016) Microglia and neuroprotection. J Neurochem 136 Suppl :10–17.

Corvino V, Geloso MC, Cavallo V, Guadagni E, Passalacqua R, Florenzano F, Giannetti S, Molinari M, Michetti F (2005) Enhanced neurogenesis during trimethyltin-induced neurodegeneration in the hippocampus of the adult rat. Brain Res Bull 65:471–477.

Deierborg T, Roybon L, Inacio AR, Pesic J, Brundin P (2010) Brain injury activates microglia that induce neural stem cell proliferation ex vivo and promote differentiation of neurosphere-derived cells into neurons and oligodendrocytes. Neuroscience 171:1386–1396.

Domercq M, Vázquez-Villoldo N, Matute C (2013) Neurotransmitter signaling in the pathophysiology of microglia. Front Cell Neurosci 7:49.

Ekdahl CT, Kokaia Z, Lindvall O (2009) Brain inflammation and adult neurogenesis:

the dual role of microglia. - PubMed - NCBI. Neuroscience 158:1021–1029.

Espinosa-Parrilla JF, Martínez-Moreno M, Gasull X, Mahy N, Rodríguez MJ (2015) The L-type voltage-gated calcium channel modulates microglial pro-inflammatory activity. Mol Cell Neurosci 64:104–115.

Fogal B, McClaskey C, Yan S, Yan H, Rivkees SA (2010) Diazoxide promotes oligodendrocyte precursor cell proliferation and myelination. PLoS One 5:e10906.

Gimeno-Bayón J, López-López A, Rodríguez MJ, Mahy N (2014) Glucose pathways adaptation supports acquisition of activated microglia phenotype. J Neurosci Res 92:723–731.

Goncalves MB, Williams E-J, Yip P, Yáñez-Muñoz RJ, Williams G, Doherty P (2010) The COX-2 inhibitors, meloxicam and nimesulide, suppress neurogenesis in the adult mouse brain. Br J Pharmacol 159:1118–1125.

Hattiangady B, Shetty AK (2008) Implications of decreased hippocampal neurogenesis in chronic temporal lobe epilepsy. Epilepsia 49 Suppl 5:26–41.

Henn MC, Janjua MB, Kanter EM, Makepeace CM, Schuessler RB, Nichols CG, Lawton JS (2015) Adenosine Triphosphate-Sensitive Potassium Channel Kir Subunits Implicated in Cardioprotection by Diazoxide. J Am Heart Assoc 4:e002016.

Humphries ESA, Dart C (2015) Neuronal and Cardiovascular Potassium Channels as Therapeutic Drug Targets: Promise and Pitfalls. J Biomol Screen 20:1055–1073.

Iwai T, Tanonaka K, Koshimizu M, Takeo S (2000) Preservation of mitochondrial function by diazoxide during sustained ischaemia in the rat heart. Br J Pharmacol 129:1219–1227.

Jaskolski F, Mulle C, Manzoni OJ (2005) An automated method to quantify and visualize colocalized fluorescent signals. J Neurosci Methods 146:42–49.

Ji R, Tian S, Lu HJ, Lu Q, Zheng Y, Wang X, Ding J, Li Q, Lu Q (2013) TAM receptors affect adult brain neurogenesis by negative regulation of microglial cell activation. J Immunol 191:6165–6177.

Kishore P, Boucai L, Zhang K, Li W, Koppaka S, Kehlenbrink S, Schiwek A, Esterson YB, Mehta D, Bursheh S, Su Y, Gutierrez-Juarez R, Muzumdar R, Schwartz GJ, Hawkins M (2011) Activation of K(ATP) channels suppresses glucose production in humans. J Clin Invest 121:4916–4920.

Kleindienst A, McGinn MJ, Harvey HB, Colello RJ, Hamm RJ, Bullock MR (2005) Enhanced hippocampal neurogenesis by intraventricular S100B infusion is

associated with improved cognitive recovery after traumatic brain injury. J Neurotrauma 22:645–655.

Koch-Weser J (1976) Diazoxide. N Engl J Med 294:1271–1273.

Liu D, Pitta M, Lee J-H, Ray B, Lahiri DK, Furukawa K, Mughal M, Jiang H, Villarreal J, Cutler RG, Greig NH, Mattson MP (2010) The KATP channel activator diazoxide ameliorates amyloid-β and tau pathologies and improves memory in the 3xTgAD mouse model of Alzheimer's disease. J Alzheimers Dis 22:443–457.

Liu F, You Y, Li X, Ma T, Nie Y, Wei B, Li T, Lin H, Yang Z (2009) Brain injury does not alter the intrinsic differentiation potential of adult neuroblasts. J Neurosci 29:5075–5087.

Lledo P-M, Alonso M, Grubb MS (2006) Adult neurogenesis and functional plasticity in neuronal circuits. Nat Rev Neurosci 7:179–193.

Mattei D, Djodari-Irani A, Hadar R, Pelz A, de Cossío L, Goetz T, Matyash M, Kettenmann H, Winter C, Wolf S (2014) Minocycline rescues decrease in neurogenesis, increase in microglia cytokines and deficits in sensorimotor gating in an animal model of schizophrenia. Brain Behav Immun 38:175–184.

Ming G, Song H (2011) Adult neurogenesis in the mammalian brain: significant answers and significant questions. Neuron 70:687–702.

Monje ML, Toda H, Palmer TD (2003) Inflammatory blockade restores adult hippocampal neurogenesis. Science 302:1760–1765.

Nakatomi H, Kuriu T, Okabe S, Yamamoto S, Hatano O, Kawahara N, Tamura A, Kirino T, Nakafuku M (2002) Regeneration of hippocampal pyramidal neurons after ischemic brain injury by recruitment of endogenous neural progenitors. Cell 110:429–441.

Ng SY, Semple BD, Morganti-Kossmann MC, Bye N (2012) Attenuation of microglial activation with minocycline is not associated with changes in neurogenesis after focal traumatic brain injury in adult mice. J Neurotrauma 29:1410–1425.

Nowakowski RS, Lewin SB, Miller MW (1989) Bromodeoxyuridine immunohistochemical determination of the lengths of the cell cycle and the DNA-synthetic phase for an anatomically defined population. J Neurocytol 18:311–318.

Ortega FJ, Gimeno-Bayon J, Espinosa-Parrilla JF, Carrasco JL, Batlle M, Pugliese M, Mahy N, Rodríguez MJ (2012) ATP-dependent potassium channel blockade strengthens microglial neuroprotection after hypoxia-ischemia in rats. Exp Neurol 235:282–296.

Ortega FJ, Jolkkonen J, Mahy N, Rodríguez MJ (2013) Glibenclamide enhances neurogenesis and improves long-term functional recovery after transient focal cerebral ischemia. J Cereb Blood Flow Metab 33:356–364.

Ortega FJ, Vukovic J, Rodríguez MJ, Bartlett PF (2014) Blockade of microglial KATP -channel abrogates suppression of inflammatory-mediated inhibition of neural precursor cells. Glia 62:247–258.

Paxinos G, Watson C (1986) The rat brain in stereotaxic coordinates, 2nd ed. Sydney: Academic Press.

Péron S, Berninger B (2015) Reawakening the sleeping beauty in the adult brain: neurogenesis from parenchymal glia. Curr Opin Genet Dev 34:46–53.

Petit P, Loubatières-Mariani MM (1992) Potassium channels of the insulin-secreting B cell. Fundam Clin Pharmacol 6:123–134.

Picard-Riera N, Nait-Oumesmar B, Baron-Van Evercooren A (2004) Endogenous adult neural stem cells: limits and potential to repair the injured central nervous system. J Neurosci Res 76:223–231.

Proks P, Ashcroft FM (2009) Modeling K(ATP) channel gating and its regulation. Prog Biophys Mol Biol 99:7–19.

Ramonet D, Rodríguez MJ, Pugliese M, Mahy N (2004) Putative glucosensing property in rat and human activated microglia. Neurobiol Dis 17:1–9.

Ribeiro Xavier AL, Kress BT, Goldman SA, Lacerda de Menezes JR, Nedergaard M (2015) A Distinct Population of Microglia Supports Adult Neurogenesis in the Subventricular Zone. J Neurosci 35:11848–11861.

Richer C, Pratz J, Mulder P, Mondot S, Giudicelli JF, Cavero I (1990) Cardiovascular and biological effects of K+ channel openers, a class of drugs with vasorelaxant and cardioprotective properties. Life Sci 47:1693–1705.

Robin E, Simerabet M, Hassoun SM, Adamczyk S, Tavernier B, Vallet B, Bordet R, Lebuffe G (2011) Postconditioning in focal cerebral ischemia: role of the mitochondrial ATP-dependent potassium channel. Brain Res 1375:137–146.

Rodríguez MJ, Martínez-Moreno M, Ortega FJ, Mahy N (2013) Targeting microglial K(ATP) channels to treat neurodegenerative diseases: a mitochondrial issue. Oxid Med Cell Longev 2013:194546.

Rodríguez MJ, Martínez-Sánchez M, Bernal F, Mahy N (2004) Heterogeneity between hippocampal and septal astroglia as a contributing factor to differential in vivo AMPA excitotoxicity. J Neurosci Res 77:344–353.

Rodríguez MJ, Prats A, Malpesa Y, Andrés N, Pugliese M, Batlle M, Mahy N (2009) Pattern of injury with a graded excitotoxic insult and ensuing chronic medial septal damage in the rat brain. J Neurotrauma 26:1823–1834.

Roseborough G, Gao D, Chen L, Trush MA, Zhou S, Williams GM, Wei C (2006) The mitochondrial K-ATP channel opener, diazoxide, prevents ischemia-reperfusion injury in the rabbit spinal cord. Am J Pathol 168:1443–1451.

Rosenblum WI (2003) ATP-sensitive potassium channels in the cerebral circulation. Stroke 34:1547–1552.

Salter MW, Beggs S (2014) Sublime microglia: expanding roles for the guardians of the CNS. Cell 158:15–24.

Sato K (2015) Effects of Microglia on Neurogenesis. Glia 63:1394–1405.

Shukry M, Kamal T, Ali R, Farrag F, Almadaly E, Saleh AA, Abu El-Magd M (2015) Pinacidil and levamisole prevent glutamate-induced death of hippocampal neuronal cells through reducing ROS production. Neurol Res 37:916–923.

Sierra A, Beccari S, Diaz-Aparicio I, Encinas JM, Comeau S, Tremblay M-È (2014) Surveillance, phagocytosis, and inflammation: how never-resting microglia influence adult hippocampal neurogenesis. Neural Plast 2014:610343.

Sierra A, Martín-Suárez S, Valcárcel-Martín R, Pascual-Brazo J, Aelvoet S-A, Abiega O, Deudero JJ, Brewster AL, Bernales I, Anderson AE, Baekelandt V, Maletić-Savatić M, Encinas JM (2015) Neuronal hyperactivity accelerates depletion of neural stem cells and impairs hippocampal neurogenesis. Cell Stem Cell 16:488–503.

Sirko S et al. (2013) Reactive glia in the injured brain acquire stem cell properties in response to sonic hedgehog. Cell Stem Cell 12:426–439.

Sofroniew M V (2009) Molecular dissection of reactive astrogliosis and glial scar formation. Trends Neurosci 32:638–647.

Solano Fonseca R, Mahesula S, Apple DM, Raghunathan R, Dugan A, Cardona A, O'Connor J, Kokovay E (2016) Neurogenic Niche Microglia Undergo Positional Remodeling and Progressive Activation Contributing to Age-Associated Reductions in Neurogenesis. Stem Cells Dev 25:542–555.

Song C, Wang H (2011) Cytokines mediated inflammation and decreased neurogenesis in animal models of depression. Prog Neuropsychopharmacol Biol Psychiatry 35:760–768.

Stebbing MJ, Cottee JM, Rana I (2015) The Role of Ion Channels in Microglial

Activation and Proliferation - A Complex Interplay between Ligand-Gated Ion Channels, K(+) Channels, and Intracellular Ca(2.). Front Immunol 6:497.

Sun D, Colello RJ, Daugherty WP, Kwon TH, McGinn MJ, Harvey H Ben, Bullock MR (2005) Cell proliferation and neuronal differentiation in the dentate gyrus in juvenile and adult rats following traumatic brain injury. J Neurotrauma 22:95–105.

Virgili N, Espinosa-Parrilla JF, Mancera P, Pastén-Zamorano A, Gimeno-Bayon J, Rodríguez MJ, Mahy N, Pugliese M (2011) Oral administration of the KATP channel opener diazoxide ameliorates disease progression in a murine model of multiple sclerosis. J Neuroinflammation 8:149.

Virgili N, Mancera P, Chanvillard C, Wegner A, Wappenhans B, Rodríguez MJ, Infante-Duarte C, Espinosa-Parrilla JF, Pugliese M (2014) Diazoxide attenuates autoimmune encephalomyelitis and modulates lymphocyte proliferation and dendritic cell functionality. J Neuroimmune Pharmacol 9:558–568.

Waclaw RR, Allen ZJ, Bell SM, Erdélyi F, Szabó G, Potter SS, Campbell K (2006) The zinc finger transcription factor Sp8 regulates the generation and diversity of olfactory bulb interneurons. Neuron 49:503–516.

Zhang R, Zhang Z, Wang L, Wang Y, Gousev A, Zhang L, Ho K-L, Morshead C, Chopp M (2004) Activated neural stem cells contribute to stroke-induced neurogenesis and neuroblast migration toward the infarct boundary in adult rats. J Cereb Blood Flow Metab 24:441–448.

Zhang X-M, Cai Y, Wang F, Wu J, Mou L, Zhang F, Patrylo PR, Pan A, Ma C, Fu J, Yan X-X (2015) Sp8 expression in putative neural progenitor cells in guinea pig and human cerebrum. Dev Neurobiol. DOI: 10.1002/dneu.22367 [Epub ahead of print].

Zhou F, Yao H-H, Wu J-Y, Ding J-H, Sun T, Hu G (2008) Opening of microglial K(ATP) channels inhibits rotenone-induced neuroinflammation. J Cell Mol Med 12:1559–1570.

FIGURE LEGENDS

FIGURE 1: Experimental groups and procedures. The different animal groups are represented as horizontal bars and grouped into three different experiments. The Dzx arrowhead in the time scale points to the day starting the diazoxide treatment. (A) For the study of the proliferation peak NMDA rats received an i.p. BrdU injection (50 mg/Kg in 50 mM PBS) on different starting days after NMDA injection (arrows) and were sacrificed at day 15 post-lesion. (B) For the study of the Dzx effects on NMDA-induced neurodegeneration rats were distributed into 10 different groups. Dzx (1 mg/kg diluted in 0.3% DMSO in water) was daily administered *per os* to rats from 4 groups (dark bars). (C) Some groups from (B) were included in the immunohistochemical study of the Dzx effects on neurogenesis (see text for details). IHQ, immunohistochemistry.

FIGURE 2: Rat glycemic measurements and determination of the NMDA-induced proliferation peak. (A) Rat blood glucose levels before and 2 hours after 1 mg/kg Dzx treatment, measured every two days. (B) BrdU-positive cell counts, with a maximal value 4 to 8 days after the lesion induction (411% vs sham, KW=1.54; p=0.017). Photomicrograph illustrates BrdU-immunostaining restricted to the cell nucleus, with irregular and dark punctuated forms corresponding to condensed chromatin. n = 6 rats/group. Scale bar 10 μm

FIGURE 3: Effect of Dzx treatment on the NMDA-induced hippocampal lesion. Microphotographs of the rat hippocampus 38 days after the injection of vehicle (sham), 20 nmol NMDA (NMDA 38 days), or 20 nmol NMDA and the oral administration of 1mg/kg/day Dzx (NMDA+Dzx 38 days). (A-C) Cresyl violet staining reveals strong neuronal loss in the NMDA and NMDA+Dzx groups, with most hippocampal layers showing great disorganization. (D-F) NeuN immunohistochemistry (IHC) shows NMDA associated neuronal loss. (G-I) Quantification of Dzx effects on NMDA-induced hippocampal lesion. Time-course study of (G) the lesioned area, and neuronal loss in (H) the pyramidal CA1 and (I) the granular layer of dentate gyrus Arrows in A-F indicate the injection site. PyrCA1, pyramidal stratum of *Cornu Ammonis* 1; grDG granular layer of the dentate gyrus. Scale bar 1 mm. n = 6 rats/group, * $p < 0.05$ different from the sham group, # $p < 0.05$ different from the NMDA group, (Bonferroni's *post hoc* test).

FIGURE 4: Effect of Dzx treatment on NMDA-induced neuroinflammation. Microphotographs of the rat hippocampus 38 days after the injection of vehicle (sham), 20 nmol NMDA (NMDA 38 days), or 20 nmol NMDA and the oral administration of 1mg/kg/day Dzx. (NMDA+Dzx 38 days). (A-C) IB4 histochemistry shows microglial reaction to the NMDA-induced lesion (D-F) GFAP immunohistochemistry (IHC) shows the astroglial reaction to the lesion. (G-H) Quantification of Dzx effects on the NMDA-induced neuroinflammation. Time-course study of the (G) area of microgliosis , and (H) the area of astrogliosis. Arrows in A-F indicate the injection site. PyrCA1, pyramidal stratum of *Cornu Ammonis* 1; grDG granular layer of the dentate gyrus Scale bar 1 mm. n = 6 rats/group, * $p < 0.05$ different from the Sham group, # $p < 0.05$ different from the NMDA group, (Bonferroni's *post hoc* test).

FIGURE 5. Proliferating cells showing glial and neuronal phenotypes 38 days after NMDA injection. Confocal images of (A) NeuN-BrdU, (C) IB4-BrdU, and (E) GFAP-BrdU double-stained cells evidenced some cells positive for BrdU and different cellular markers (arrowheads)**.** Histograms showing the number of (B) double Brdu-NeuN, (D)BrdU-IB4, and (F) BrdU-GFAP ico-expressinge cells 38 days post-lesion, in the different layers of the hippocampal formation. (G) Relative number of neurons (NeuN), astrocytes (GFAP), and microglia (IB4) double-stained BrdU-positive cells in the entire HF. SGZ, Subgranular zone; Par, hippocampal parenchyma. n = 6 rats/group, * $p < 0,05$ different from the Sham, group # $p < 0,05$ different from the NMDA group (Bonferroni's *post hoc* test). Scale bar 20μm.

FIGURE 6: Most DCX-immunopositive cells are BrdU negative. Confocal images of DCX-BrdU co-localization in (A-C) the SGZ and (D-F) the lesioned hippocampus 15 days after NMDA injection. Histograms show numbers of (G) DCX-immunopositive cells and (H) BrdU-DCX-immunoreactive cells on day 15 post-lesion. SGZ, subgranular zone; hipp, hippocampus. * $p<0.05$ different from the sham group (Bonferroni's *post hoc* test). Scale bar 50 μm. Inset scale bar 10 μm.

FIGURE 7: Localization of Sp8-positive cells in the lesioned hippocampus. Photomicrographs of the (A) control hippocampal formation and (B) SVZ, and (C,D) of the NMDA-lesioned hippocampus. (E,F) Photomicrographs of immunofluorescent Sp8

staining illustrate differences between the hippocampus of NMDA-lesioned rats and NMDA+Dzx rats, 15 and 38 days after the lesion. (I) Numbers of Sp8 positive cells in the hippocampus of sham, NMDA and NMDA+Dzx rats. CA1, Cornus Ammonis 1; DG, dentate gyrus; LV, Lateral ventricle. n = 6 rats/group. # $p < 0,05$ when compared to day 15 post-lesion (Bonferroni's *post hoc* test). Scale bar 500 µm for A and C; 100 µm for B and D; and 1 mm for E-G .

FIGURE 8: Sp8 expression in GFAP-immunopositive cells. (A-C) Confocal images of NeuN and Sp8 double staining in the hippocampus of NMDA-lesioned rats. (D) Confocal image of an XY plane with the merged channels, (E) the MDP map showing the colocalization map of the red and green channels, and (F) the scatter plot from the merged image. (G-I) Confocal images of GFAP and Sp8 double staining in the hippocampus of NMDA-lesioned rats. (J) Confocal image of an XY plane with the merged channels, (K) the MDP map and (L) the scatter plot from the merged image. In the scatter plots, the green channel intensity increases from left to right on the X-axis, and the red channel intensity increases from bottom to top in the Y-axis. The absence of yellow dots in (E) and (F) denotes no colocalization of the two channels. The presence of yellow dots in (K) and (L) denotes colocalization of the two channels. Scale bar, 40 µm.

Table 1: Primer and probe sequences for real-time RT-PCR

Target	Gene	Sequence (5'-3')	Size (bp)	Accesion Nº
GAPD	rat Gapd	F: AGA CAG CGC ATC TTC TTG T R: CTT GCC GTG GGT AGA GTCAT	207	NM_017008
Kir 6.1	rat Kcnj8	F: CAC AAG AAC ATC CCG AGA GCA R: CGT GAA TGA CCT GAC ATT GG	246	NM_017099
Kir 6.2	rat Kcnj11	F: CCA CCC ATT CTC TGT CTG TC R: CCA GGA TTT GAA CCA ATC CAG	166	NM_031358
SUR 1	rat Abcc8	F: TGA ACA CAG CTA TCC CCA TT R: CTC TGC ACT GGA CAG GAA CT	218	NM_013039
SUR 2	rat Abcc9	F: CCA ACA TCG TCT TTT TGG AC R: AAC ACA CTG CCA TCC TTC AT	184	NM_013040

Table 2. K_{ATP} channel gene expression in NMDA-lesioned hippocampus

Gene	Group	Fold change vs sham	95% CI	p-value
Kir6.1	NMDA 5 days	2.596	1.88 - 3.31	0.009
	NMDA 15 days	0.477	0.25 - 0.75	0.32
	NNMDA 38 days	0.968	0.51 - 1.43	0.91
	NMDA+Dzx 15 days	1,573	0.17 - 2.97	0.33
	NMDA+Dzx 38 days	1,469	1.02 - 1.91	0.35
Kir6.2	NMDA 5 days	1.766	0.83 - 2.7	0.19
	NMDA 15 days	0.733	0.41 - 0.57	0.54
	NNMDA 38 days	1.054	0.92 - 1.19	0.92
	NMDA+Dzx 15 days	1.267	0.08 - 2.45	0.67
	NMDA+Dzx 38 days	2.236	1.36 - 3.10	0.07
SUR1	NMDA 5 days	1.189	0.61 - 1.77	0.56
	NMDA 15 days	0.440	0.31 - 0.57	0.16
	NNMDA 38 days	0.944	0.85 - 1.04	0.99
	NMDA+Dzx 15 days	1.027	0.44 - 1.61	0.84
	NMDA+Dzx 38 days	1.585	0.31 - 2.85	0.29
SUR2	NMDA 5 days	2.218	1.35 - 3.09	0.007
	NMDA 15 days	1.484	0.80 - 2.16	0.13
	NNMDA 38 days	0.945	0.04 - 1.84	0.98
	NMDA+Dzx 15 days	1.101	0.12 - 2.08	0.69
	NMDA+Dzx 38 days	2.470	0.50 - 4.43	0.046

CI, Confidence interval.

FIGURE 1: Experimental groups and procedures.

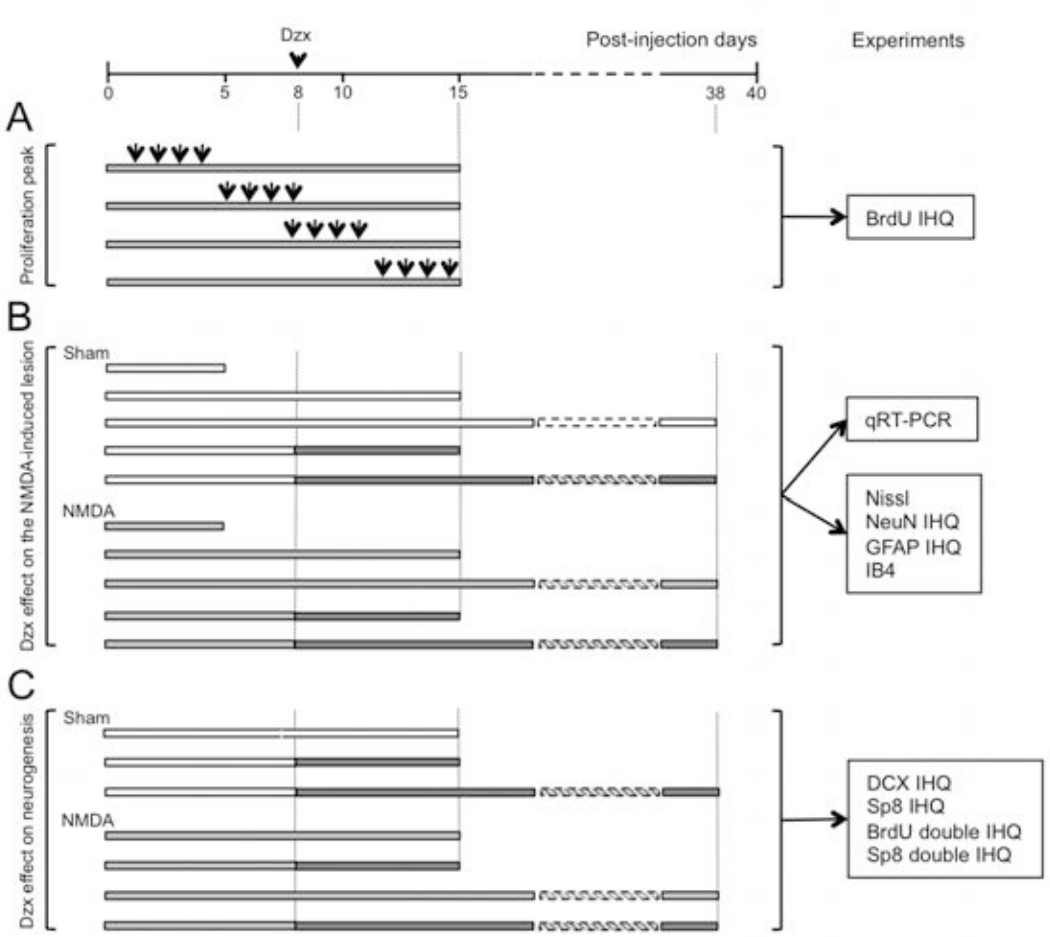

FIGURE 2: Rat glycemic measurements and determination of the NMDA-induced proliferation peak.

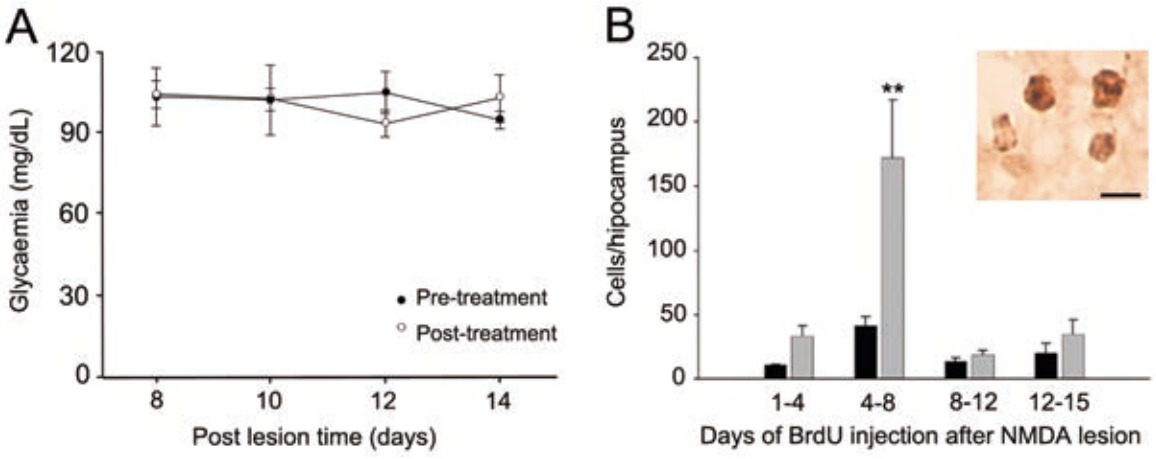

FIGURE 3: Effect of Dzx treatment on the NMDA-induced hippocampal lesion

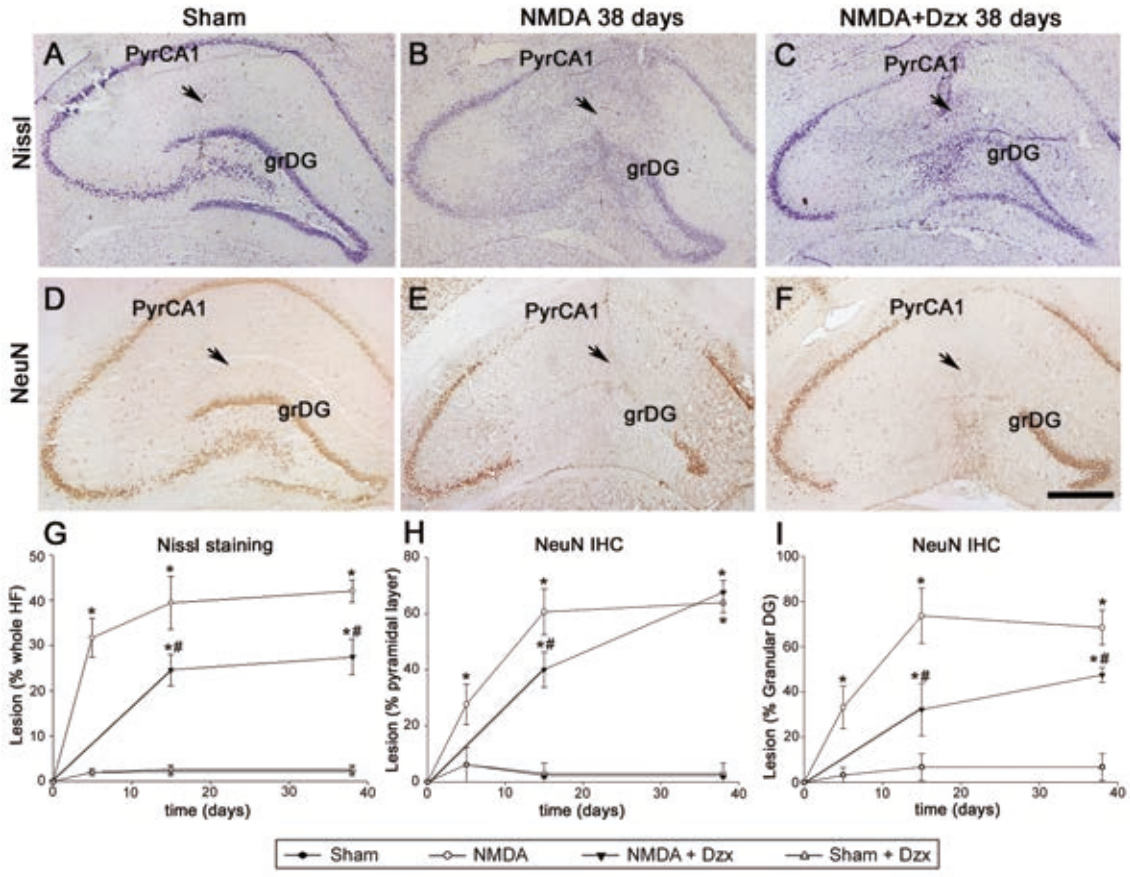

FIGURE 4: Effect of Dzx treatment on NMDA-induced neuroinflammation

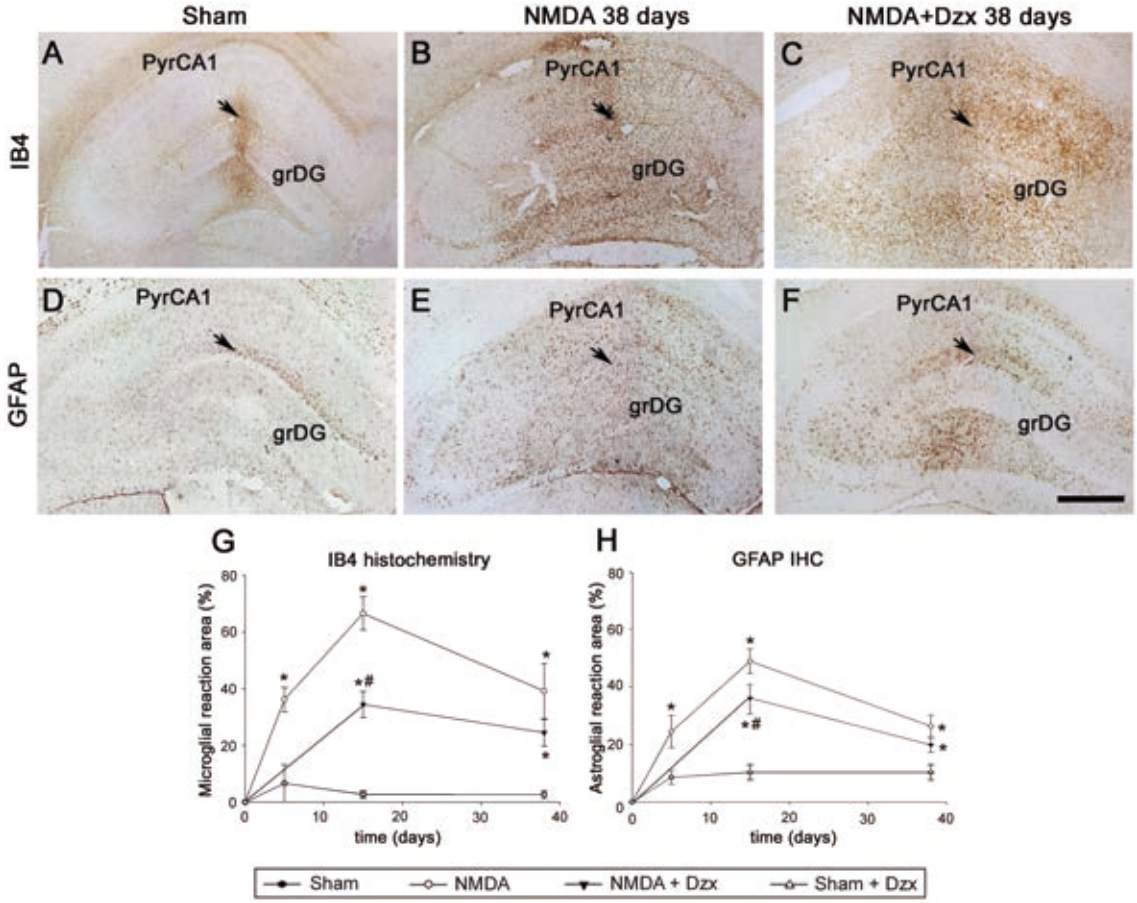

FIGURE 5. Proliferating cells showing glial and neuronal phenotypes 38 days after NMDA injection

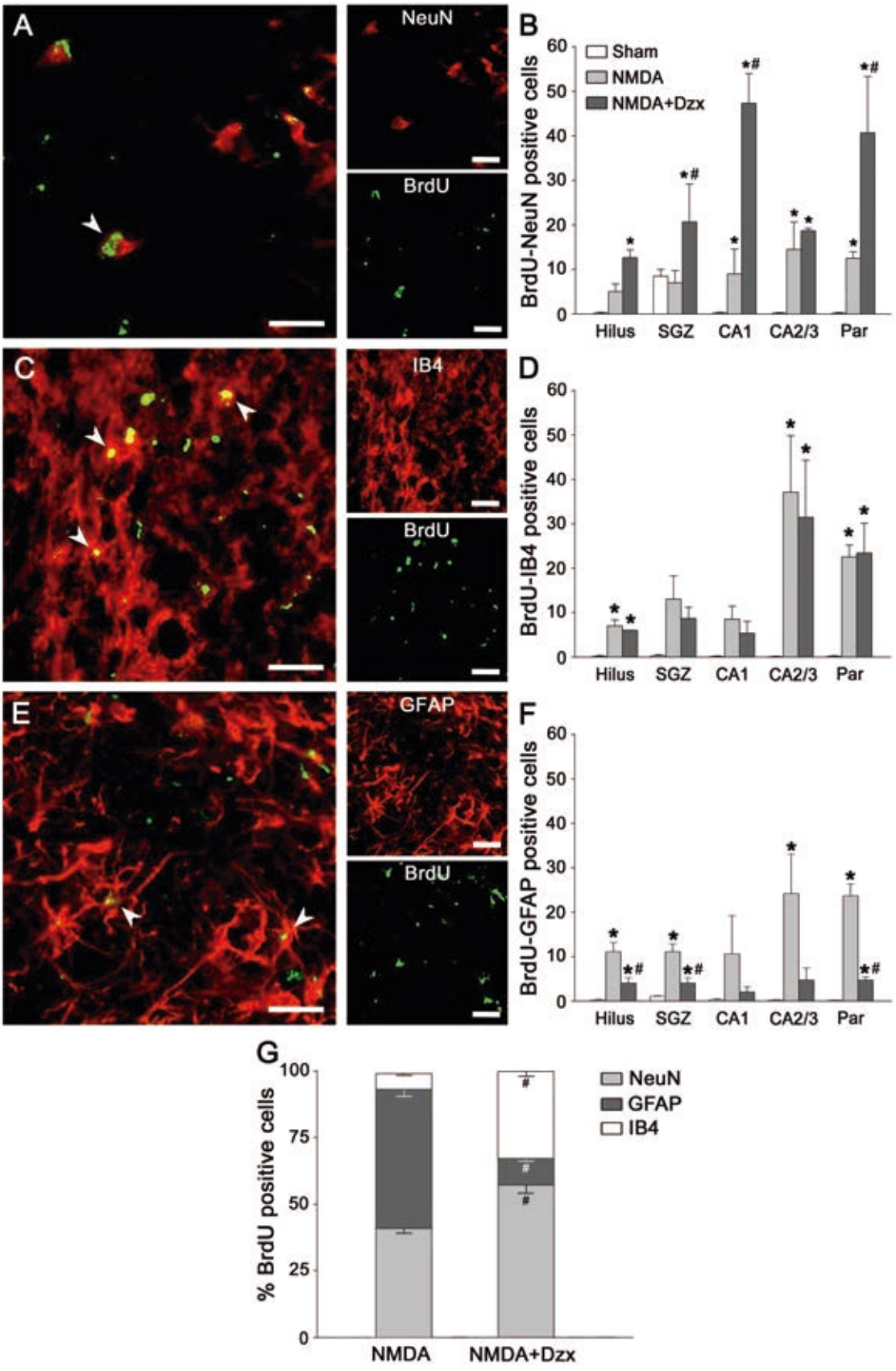

FIGURE 6: Most DCX-immunopositive cells are BrdU negative.

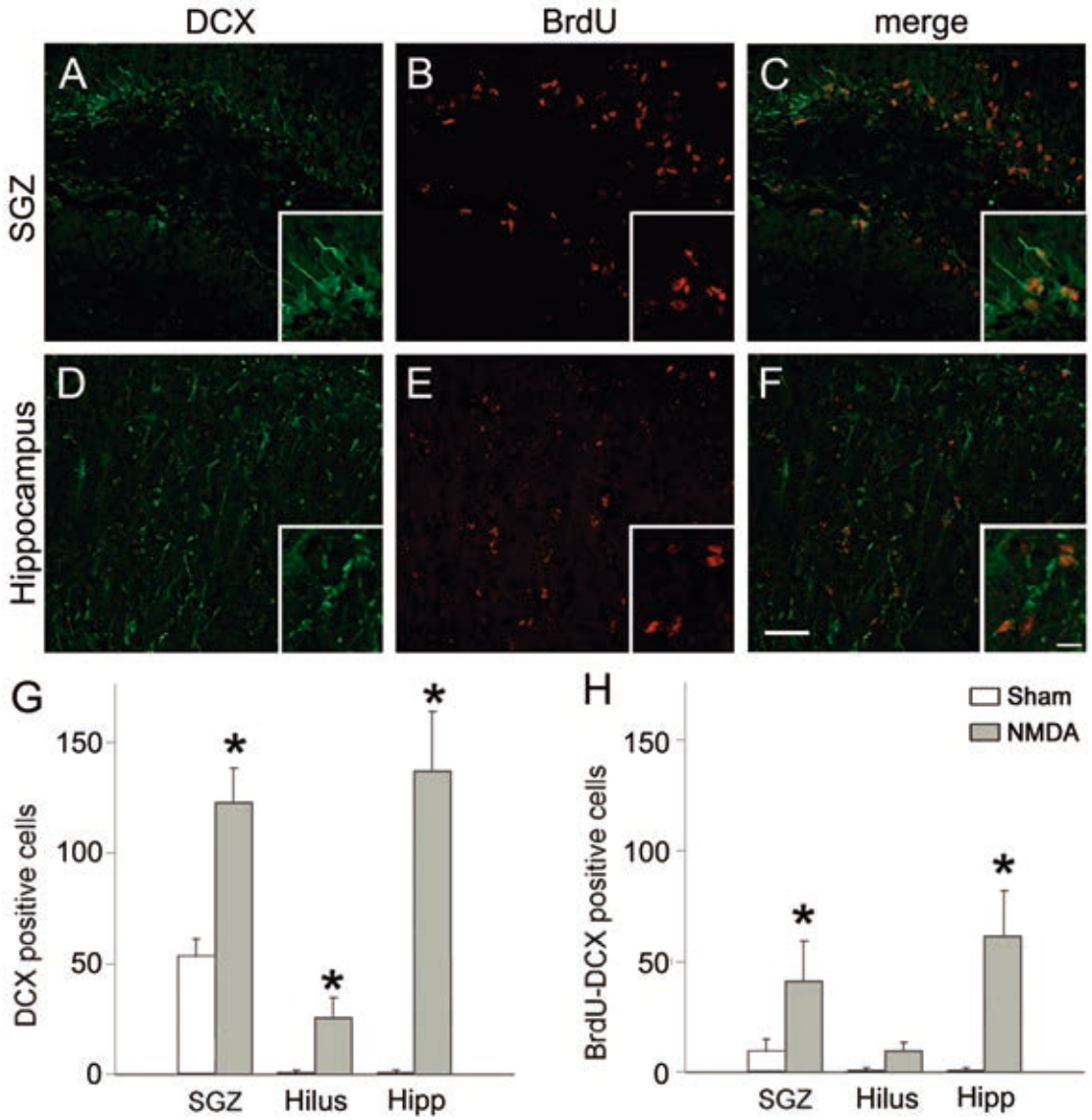

FIGURE 7: Localization of Sp8-positive cells in the lesioned hippocampus

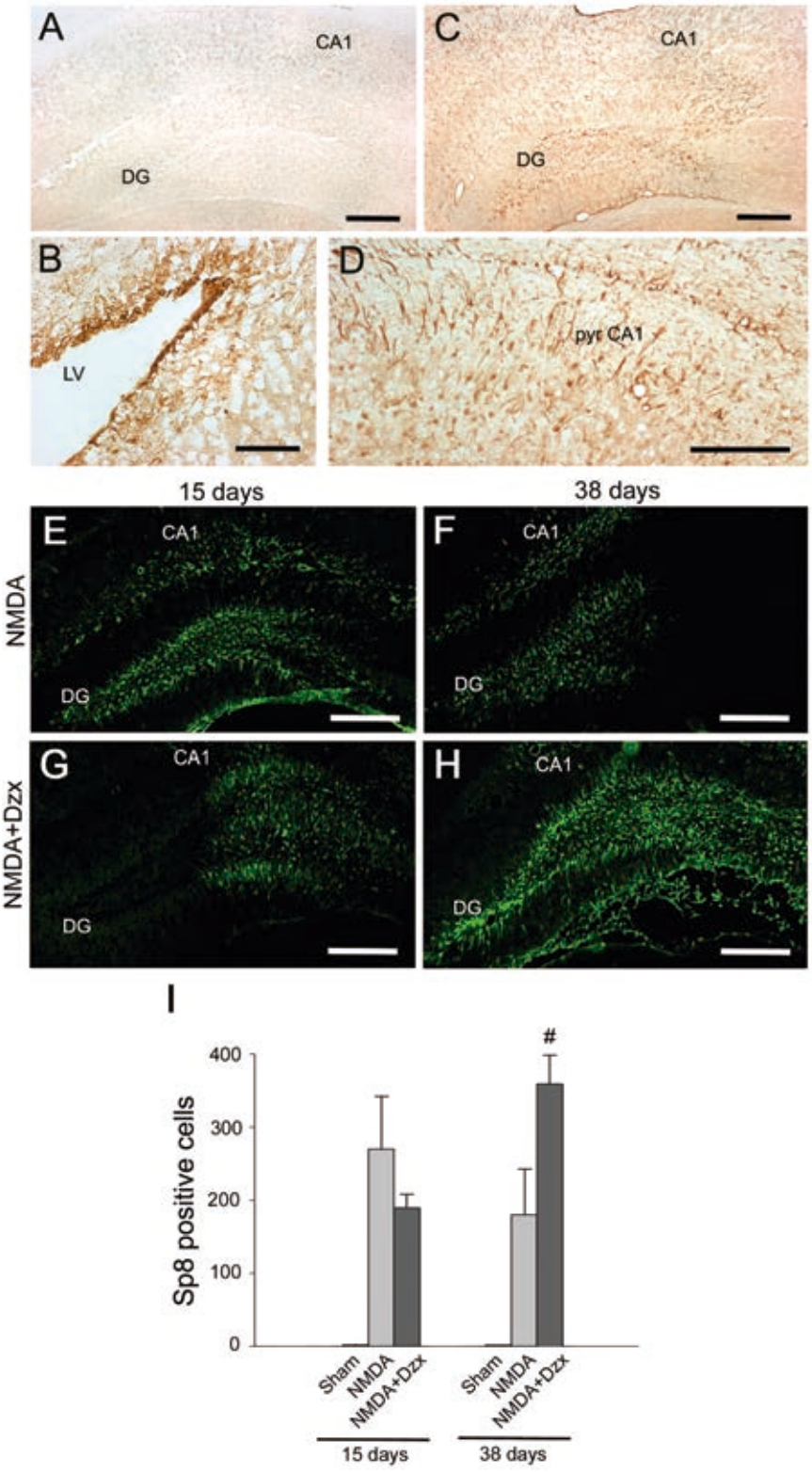

FIGURE 8: Sp8 expression in GFAP-immunopositive cells